SALTY TREE-RINGS: USING POTENTIAL IMPURITY LAYERS WITHIN EUROPA'S ICE SHELL TO INFER RESURFACING HISTORY. E. J. Leonard[1] and S. Howell[1], [1]Jet Propulsion Laboratory, California Institute of Technology (Erin.J.Leonard@jpl.nasa.gov)

Introduction: Europa, a Galilean moon of Jupiter, possesses an outer water ice shell 3-30 km thick that overlays a saltwater ocean ~100 km deep. The icy surface of Europa records a complex history of tectonic deformation, including the exposure of interior ice at extensional bands and removal of surface material to the interior at inferred subsumption zones [1, 2]. These geologic processes are critical for transporting material through the brittle ice shell exterior [2, 3] and understanding the redox state and astrobiological potential of the interior ocean [4]. Some tectonic features are associated with the exposure of more non-ice materials than their surroundings [5], indicating spatial or temporal variations in the distribution of impurities within the ice shell.

Changes in ice shell thickness with time is one process that could be driving surface deformation on Europa. Ice shell thickness changes induce large stresses at low strains [2, 6]. As the ice thickness changes, the amount of non-ice material incorporated into the ice from the ocean depends to first-order on how quickly the ocean freezes [7]. Therefore, the distribution of non-ice materials may reflect the evolution of the ice shell as it thickened and new material froze in. Later tectonic processes may deform the ice shell, sampling compositional variations that are then exposed at the surface.

In order to understand what compositional variations may arise from a thickening ice shell and the associated surface exposure, we numerically model ice shell evolution and deformation [2]. We simulate the interaction between an outer ice shell and a mock interior ocean to create cross-sectional maps of historical freezing rate at the time of ice incorporation to the shell. Using freezing rate as an analog for non-ice incorporation, we infer the distribution of non-ice impurities within the ice shell.

Observations: Europa's young average surface age (40-90 Myr) indicates recent or extant resurfacing processes [e.g., 8]. Observations of the cross-cutting relationships of surface features indicate that deformation style has evolved throughout Europa's visible surface history, from forming ridged plains early on, to tabular bands, and finally to chaos and crack formation [9, 10]. Based on the inferred formation mechanisms for each of these terrains [10], the deformation of the ice shell has progressed from distributed to discrete. This progression of deformation, could indicate that the ice-shell has thickened throughout its visible surface history [9, 10]. If ice-shell thickening events are recurrent throughout Solar System history (e.g., due to potential changed in orbital eccentricity) [e.g., 11] we hypothesize that thickening events may be recorded in the distribution of non-ice materials within the ice-shell and on the surface.

The distribution of non-ice materials across Europa's surface is non-uniform and, in most cases, higher concentrations of salt occur in discrete regions associated with geologic structures such as bands and chaos (Fig. 1) [5]. Therefore, non-ice features on Europa's surface may be linked to the exposure of material originating in the ice shell or subsurface ocean.

Methods: In this study, we focus on the geologic transport of ice shell material by building on the modeling approach of Howell and Pappalardo (2018). We extend the finite element code SiStER (Simple Stokes solver with Exotic Rheologies) [2, 12] to simulate the visco-elasto-plastic behavior of ice I above a simulated ocean (Fig. 2). We include partial melting and freezing [13] that affects the density and mechanical behavior of particles within the finite difference mesh. For particles transitioning from the ocean to the ice shell, we record the maximum freezing rate ever experienced as an indicator of potential impurity incorporation. The model includes internal tidal heat generation and basal silicate heat flux to the ocean.

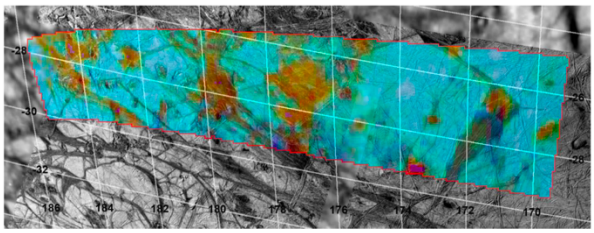

Figure 1: The concentration of non-ice materials is indicated by the color, where blue is lower and warmer colors are higher. Note the apparent association of non-ice materials with band and chaos terrains. Modified from Prockter et al. (2017) Fig. 2.

We investigate 3 scenarios for ice-shell evolution:

Freeze-in. An ice shell freezes in from an ocean exposed to space. In this case, we predict an impurity-rich layer at the surface, and a gradational decrease in non-ice abundance with depth (Fig. 2, top).

Thaw-out. An initial 130 km thick shell thins. While the lithosphere retains its primitive composition, a convecting interior may permanently incorporate ocean material (Fig. 2, bottom).

Varying thickness. A frozen-in ice shell thickens or thins in response to a change in heating. Here, multiple non-ice horizons are recorded within the ice shell.

We also investigate the lateral variations in composition due to extension and compression. A frozen-in ice shell will exhibit extensional bands with lower non-ice abundances (Fig. 3, top). A thawed-out shell will exhibit bands with moderate non-ice abundances. A layered shell may exhibit lateral horizons in non-ice abundances. Compression thickens the lithosphere, and results in locally thicker impurity layers for a frozen-in shell (Fig. 3, bottom).

Geological Implications: In the extensional bands scenario, assuming the ice shell undergoes freeze-in, models predict less salt in the ice at the band center than in the surrounding terrain. This is contradictory to observations of Europa's surface (e.g., Fig. 1). However, sputtering and radiation effects on the older surface may be hiding the saltier material we would expect to observe. If this is the case, the planned NASA Europa Clipper spacecraft's REASON radar instrument may be able to observe changes in electrical conductivity associated with changes in salt content. For example, an extensional band may exhibit a lower inferred salt content (lower dielectric constant) in the ice shell beneath the band center than beneath the immediately surrounding area. At subsumption zones, a thicker layer of inferred salt concentration within the ice shell compared to the surrounding area may indicate deformation of salt-rich layers from thickening events.

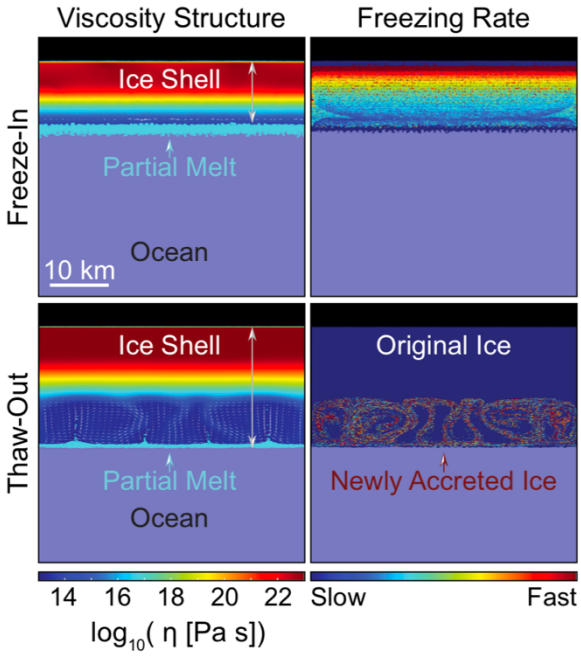

Figure 2: 2-D model predictions of (left) viscosity structure and (right) freezing rate at the time of incorporation into the ice shell for a case in which the ice shell froze in from 500 m initial thickness (top) and a case where the ice shell thawed out from 130 km initial thickness (bottom). Rates vary from 1% to 10% change in melt content per thousand years.

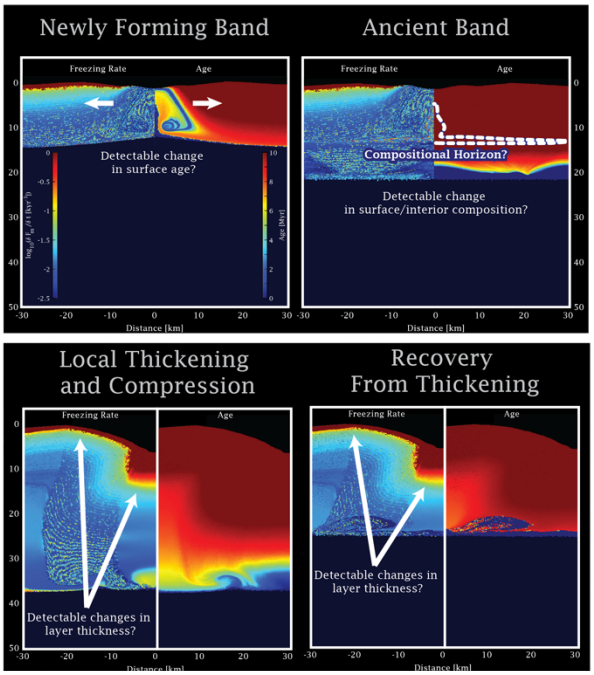

Figure 3: Top: Extension in the freeze-in model. Note the change in composition (freezing rate) and age in the exposed ice. Bottom: Compression in the freeze-in model.

Conclusions: We infer spatial and temporal changes in Europa's ice shell composition from models of freezing rate of ocean water at the time of incorporation into Europa's ice shell. As tree rings provide an insight into the seasonal environment at the time of wood growth, we interpret these predictions of inferred global brine horizons to reflect the accretion history of incorporated ice. Non-ice distributions may record geologic history and interior heat flux, and might constrain whether the ice shell interior is convecting. Future robotic exploration missions to ocean world ice shells, like NASA's planned Europa Clipper mission and ESA's planned JUICE mission, may test whether such thickening events are recorded by compositional variations within the ice shell.

References: [1] Kattenhorn, S. A., Prockter, L. M. (2014) *Nat. Geosci.*, 7, 762–767. [2] Howell, S. M. & Pappalardo, R. T. (2016) *GRL,* 45, 4701–4709. [3] Howell, S. M., Pappalardo, R. T. (2019) *Icarus*. [4] Hand, K. P. et al. (2009) *Europa*, pp 589. [5] Prockter, L. M. et al. (2017) *Icarus*, 285, 27–42. [6] Nimmo, F. (2004) *JGR Planets*, 109. [7] Ozum, B., Kirwan, D. J. (1976) *AIChE Symp Series*, 153, 1–6. [8] Bierhaus, E. B. and Chapman, C. R. (2009), in *Europa*, pp. 161–180. [9] Figueredo, P. H. and Greeley, R. (2004) *Icarus*, 167, pp. 287–312. [10] Leonard, E. J., Pappalardo, R. T. and Yin, A. (2018), *Icarus*, 312. [11] Ojakangas, G. W. and Stevenson, D. J. (1986) *Icarus.* [12] Olive, J.-A. et al. *GJI*, 205, 728–743. [13] Tobie, G., Choblet, G., Sotin, C. (2003) *JGR Planets*, 108.